CCFE

CULHAM CENTRE FOR FUSION ENERGY

UK Atomic Energy Authority

UKAEA-CCFE-PR(22)18

T. Eade, S. Bradnam, P. Kanth

A new novel-1-step shutdown dose rate method combining the benefits of the rigorous-2-step and direct-1-step methods

A new novel-1-step shutdown dose rate method combining the benefits of the rigorous-2-step and direct-1-step methods

T. Eade, S. Bradnam, P. Kanth

A new novel-1-step shutdown dose rate method combining the benefits of the rigorous-2-step and direct-1-step methods

T. Eade[a], S. Bradnam[a], P. Kanth[a]

[a]Culham Centre for Fusion Energy, Culham Science Centre, Abingdon, UK

Abstract

A new method for the calculation of Shutdown Dose Rates (SDDR) has been developed, the Novel-1-Step (N1S) method. The new method retains the benefits of only requiring a single radiation transport calculation, as in the use of the direct-1-step (D1S) method, while removing the need for pre-calculations to determine dominant nuclides and time correction factors. The N1S method uses a time dependent source and decay data for all isotopes. When reactions in the transport occur leading to unstable daughter nuclide, the correct contribution of photon radiation from all the decay products of a nuclide are calculated with no need for additional external activation calculations. Weights of these decay photons are calculated for each decay time of interest and are analytically calculated based on the solutions to the Bateman equations.

The N1S method has been implemented into MCNP and preliminary verification calculations performed. These calculations included the FNG ITER shutdown dose rate benchmark and the ITER SDDR cross comparison. For the FNG ITER SDDR benchmark the N1S method showed good agreement, within experimental error, for the first campaign apart from the first decay time where a C/E value of 1.34 was obtained. This was shown to be due to the decay of ^{64}Cu inside the copper cup of the neutron generator. For the second campaign the N1S method showed an under prediction of up to 20% at short decay times and an over prediction up to 20% at longer decay times. These times are dominated by ^{56}Mn and ^{58}Co respectively and it is likely the difference is due to under and over predictions in the reaction rates leading to these isotopes. The ITER cross comparison showed good agreement between the N1S method and MCR2S (and by association other D1S and R2S codes). Difference seen in the results were shown to be due to difference in the calculated reaction rates using EAF2010, TENDL2019 and FENDL3.2.

Keywords: N1S, MCNP, Neutronics, Shutdown Dose, ITER, FNG

1. Introduction

An important consideration as fusion moves from relatively low power research reactors to electricity producing power plants is the resulting increase in the neutron yield and the subsequent radiation fields produced. Power reactors will require a significant increase in the Deuterium-Tritium (D-T) reaction rate leading to significantly more 14.1 MeV neutrons being produced. These 14.1 MeV neutrons will not only create a radiation field during operation but also activate materials leading to significant photon radiation fields as unstable isotopes decay during shutdown. This can pose a significant radiation hazard to personnel and remote handling equipment during maintenance, as well as impacting the level of nuclear waste and decommissioning strategies at the end of the plants life. It is therefore vital that these shutdown radiation fields are well understood and taken into account during the design of the reactor and maintenance procedures.

Two main approaches to calculating the radiation levels in fusion reactors during shutdown are currently used. The first being the direct-1-step method (D1S) and the second being the rigorous-2-step (R2S) method. These both have advantages and disadvantages.

Two implementations of the D1S method [1][2] have been developed with various capabilities, but are both based on the same underlying principles and implemented into modified versions of the Monte-Carlo N-Particle (MCNP5[3] & MCNP6 [4]) code with specially prepared nuclear cross-section data [1]. This bespoke nuclear cross-section data swaps out information in the MCNP ACE (A Compacted ENDF) files used for the creation of prompt gammas and replaces it with data on the creation of decay gammas. This allows the interaction of neutrons with matter and, the creation and transport of decay gammas to be incorporated into a single transport calculation. With this approach, decay gammas are modelled in situ, eliminating the need to spatially discretise the geometry as the gammas are started in the location of reaction. This method also inherently takes self-shielding into account as the flux and spectrum do not have to be discretised over space and energy domains. One disadvantage of the D1S method is its use of 'time correction factors' as it does not use a time-dependent transport calculation. These time correction factors are pre-requisites for a given nuclide and thus require pre-calculation. This means prior knowledge of the nuclides that dominate the nuclear response of interest is required and pre-calculation of the time correction factors carried out with an inventory code such as FISPACT-II [5]. This fundamental requirement for a priori knowledge of the dominant nuclides giving rise to the nuclear field, could lead to incorrect results when applying the technique generally.

Several R2S implementations have been developed over the past decade [6][7][8][9]. Unlike the D1S approach the R2S approach is carried out in multiple calculation steps involving a radiation transport code and an inventory code. The transport code is used to calculate the spatially varying neutron flux and spectra around the model geometry. This spatially varying neutron flux and spectra is discretised into an average value for a given volume and recorded in tallies, which can take the form of cell tallies (which record the averaged neutron flux and spectrum in the geometrical cells which make up the model) or, more usually, super imposed mesh tallies (which record the average flux in regularised voxels across the entire geometry). In either case the neutron flux and material information is then passed to the inventory code where explicit activation calculations are carried out for each cell or voxel. The gamma intensity and spectrum from these inventory calculations are then used to build a source term for a final radiation transport calculation to ascertain the gamma field and shutdown responses around the geometry. Some of the advantages of the R2S method are no prior knowledge of the dominant nuclides is required, other nuclear responses (such as activity, decay heat, inventories etc) can be acquired from the activation calculations, changes to the model can be made between the neutron and photon transport simulations, and the irradiation scenarios can be changed without the need to re-run the neutron transport calculation. The main disadvantage of the R2S approach is the need to discretise into bins the spatial and energy distribution of the neutron flux, this leads to flux averaging which can lead to under and over prediction of the gamma source in certain regions. The R2S method also requires more analysts time as three separate calculation steps (neutron transport, activation and photon transport) are required to be set up and run. It also requires separate photon transport calculations to be carried out for each decay time of interest.

This paper documents a novel solution in the form of the Novel-1-Step (N1S) method, to negate some of the disadvantages inherent in the D1S and R2S codes. The N1S method retains the advantages of the D1S calculations, including being carried out in a single transport calculation with absolute spatial and energy treatment of reactions, while removing the disadvantage of requiring pre-analysis to determine the dominant nuclides. This removes the possibility of human error in missing important isotopes as all isotopes are included. It also means that the N1S system could be included in automated workflows more easily as no input from an analyst is required.

Along with a description of the N1S methodology given in Section 2 this paper also details some preliminary benchmarking of the N1S methodology using the FNG ITER Shutdown Dose Rate Benchmark in Section 3.1 and the ITER SDDR cross comparison in Section 3.2.

2. N1S Method

2.1. Overview

Like the D1S method the N1S method is carried out within a single transport calculation. However, unlike the D1S method,

a time-dependent transport calculation is required. This means that the irradiation schedule is taken into account with a time dependent neutron source, thus removing the need for time correction factors. When neutrons interact with a parent nuclide which produces an unstable daughter, the N1S library is called to sample the decay gammas and optional x-rays associated with the daughter. Information on these decay photons is then passed back to the transport code and the decay photons are added to the banked particle list to be transported. The N1S library also calculates a set of weights for each of the decay photons. The number of weights is equal to the number of decay times in the problem. These weights are calculated based on the probability of the isotope (and subsequent isotopes in the decay chain) decaying at the decay times of interest. These weights are then used to modify the response of the tallies at the decay times of interest for each of the decay photons that make it to the tally. A flow diagram depicting the N1S process is given in Figure 1.
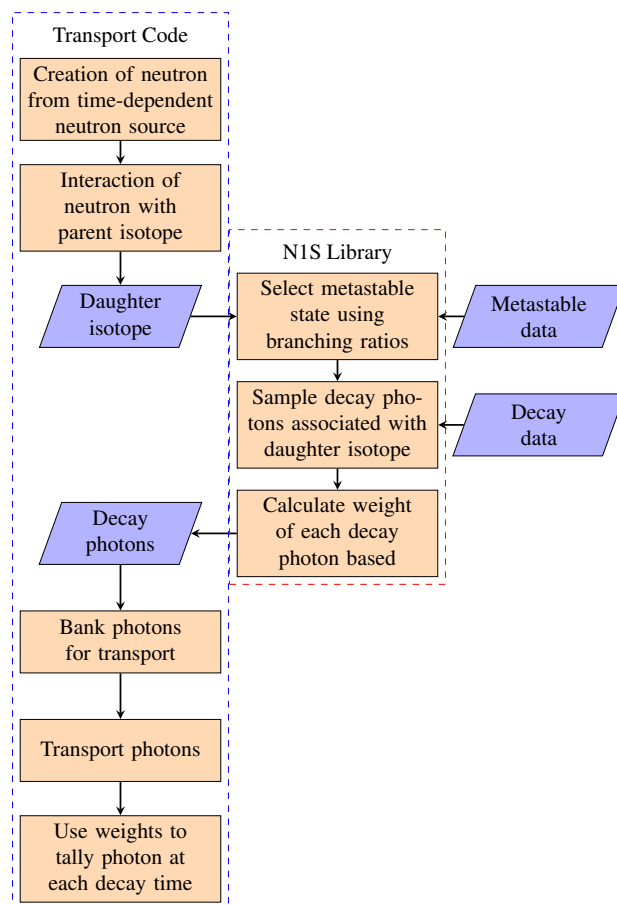
Figure 1: Overview of the basic N1S process

The following three sections give more details on the decay data used and how it is stored, the handling of metastable states which are not inherently tracked in transport codes such as MCNP and the sampling routines used for sampling decay photons.

2

2.2. Decay library

The main advantage of N1S method over the D1S method is the accurate simulation of decay of radioactive isotopes and sampling of photons from the all decay products. The data needed to simulate this and solve the Equation 2 is obtained from an ENDF-6 format [10] decay data library. Currently two versions of this decay library are available 2012 [11] and 2020 [12]. The decay data includes the decay mode of the isotopes, radiation type emitted during each decay, and the energy and relative intensity of each emitted radiation. Since only the photon spectrum is important for shutdown dose rate calculations, the energy and the intensity of each photon line (gamma and x-rays) is stored. The N1S decay data reader goes through the files for each individual isotope and extracts the half-life, number of decay modes and spectral information given in the file. It then extracts the energy and relative intensity of each photon line given in the data file. One current limitation of the N1S method is it is only able to read discrete spectra given in the decay data library and not the continuous spectra, which are available for some isotopes with high mass number. As these high mass number isotopes are not generally used in fusion applications this current omission will not effect its applicability to fusion problems. However, an addition to read in and sample continuous spectra will be added at a later date to increase the completeness of the N1S method and increase the applicability of the N1S method outside of fusion.

The program calculates and stores the cumulative photon distribution for each isotope, from which the photon will later be sampled. The program also calculates the daughter product of each decay mode and the decay constant for the mode of decay. If an isotope decays via two decay modes, for example, ^{48}Ca decays by either single beta decay to ^{48}Sc or double beta decay to ^{48}Ti with 50% branching ratio for each decay mode, the program stores the daughters produced and the branching ratio for the production of each daughter product. These quantities are then used by the sampling routine explained in Section 2.4.

2.3. Meta-stable states

Meta-stable states caused from reactions are not taken into account in transport codes as they have a negligible impact on the particle transport. Older versions of the ACE (A Compact ENDF) nuclear data files and MCNP, only support proton and mass numbers (ZAIDs) of format ZZZAAA which does not include information on the metastable states. Although modifications have been made to the ACE data format [13] to take account of metastable states and support has been added to MCNP6; this only allows metastables to be specified in the material definition. The N1S method requires information on the daughter products from reactions which is not available. Therefore in order to capture the production of all metastable states in daughter isotopes an additional capability has been added to the N1S workflow. In the case of the FENDL3.2 cross section library, it contains point wise total production cross section data for a given reaction channel, so a branching ratio factor must be derived to determine the production rate of each metastable state for a given interaction.

The fraction of mestastable daughter produced is inherently linked to the incident neutron energy of the interaction. Utilising the Fortran Application Programming Interface (API) for FISPACT-II, groupwise cross section data can be parsed from ENDF-6 [10] or legacy EAF [14] formatted files, and easily accessed using a number of inbuilt subroutines. A utility program has been written which loops through all stable ground state parent isotopes in a given library, cycling through all possible reaction channels and extracting the daughter proton number, atomic mass, isomer (ZAI). In the ENDF-6 files the last digit of the ZAI indicated the state, for example, 0 would be a ground state isotope, 1 would be the first metastable state, etc. Therefore for any reaction channels where a metastable daughter isotope is possible, the groupwise cross section data is stored for all possible states and resized to be equal length for any products which may have threshold production energies. This data is re-normalised for each energy bin, producing a cumulative probability distribution for state production as a function of energy. These cumulative probability distributions are output to a binary data file which can be used in N1S calculations. As this metastable binary file contains data on all isotopes it only needs to be created once and then can be used in all subsequent N1S calculations.

The metastable data file to be used can be specified at run time and the N1S routines read this data in. Once the data has been read into memory as a hash table it can then be sampled to ascertain the state of a daughter isotope. To do this a subroutine has been added to the N1S workflow, which requires the parent ZAID, reaction MT number and incident neutron energy. The metastable sampling routine uses the cumulative probability distribution for the energy bin in which the neutron energy falls and a random number to sample which state the daughter isotope is in. The daughter ZAI is then passed on to subsequent photon sampling routines described in Section 2.4.

2.4. Sampling routines

When a reaction occurs in the transport code the parent ZAID, MT reaction number, neutron energy and decay times are passed to the N1S library. The library first selects the daughter ZAI using the metastable sampling routine described in Section 2.3. Once the daughter ZAI has been found this is passed to the sample photon routine along with the decay times to sample the photons to start and calculate their weight.

For a given daughter decay the number of photons sampled is based on the sum of the relative intensities. Equation 1 is used to select the number of photons to start for a given decay.

$$N_{photons} = \left\lfloor R + \sum_{i=1}^{n} I_i \right\rfloor \tag{1}$$

Where $N_{photons}$ is the number of photons sampled for the given decay, R is a random number between 0 and 1, n is the number of photon lines for the daughter and I_i is the relative intensity of photon line i.

If this daughter is in a decay chain the code also samples the photons associated with any nuclide in the chain. To work out the nuclides to sample the N1S method uses a linear decay chain

solver [15]. This chain solver breaks complex decay chains up into a series of linear decay chains which can then be easily manipulated. The decay chain solver creates linear chains for a given nuclide by doing a depth first search using a recursive algorithm. These photons are then banked for transport once the tracking of the primary particle has finished.

The sampling of the photon energies is analogous to the process that occurs in nature; however if like nature these decay photons were started at decay times randomly based on the half-life of the daughters it is unlikely that sufficient statistics at a specific decay time of interest would be obtained for a typical nps of around 1e9. To get around this, the N1S method works out the probability of a given decay photons starting at each of the decay times of interest (i.e. the decay times associated with the tallies in the problem). This probability for each of the daughters in the decay chain is based on the solution to the Bateman equations [16] given in by Equation 2 [15].

$$A_n(t) = N_1(0) \sum_{i=1}^{n} \lambda_i \alpha_i \exp[-\lambda_i t] \qquad (2)$$

Where A_n is the activity of the nth daughter in the chain, $N_1(0)$ is the number of first atoms of the first isotope in the chain at $t = 0$, λ_i is the decay constant of the ith daughter in the chain, t is the time at which the the activity is to be found and α_i is given by Equation 3.

$$\alpha_i = \prod_{\substack{j=1 \\ j \neq i}}^{n} \frac{\lambda_j}{\lambda_j - \lambda_i} \qquad (3)$$

Instead of the activity the N1S method actually needs the likelihood, $P_n(t)$, of the decay occurring at time t. Where time t is the difference in time between the reaction occurring and the time of interest. To get the likelihood we set the number of atoms of the first isotope in the chain to be 1 at $t = 0$ (i.e. the time of the reaction). This gives Equation 4.

$$P_n(t) = \sum_{i=1}^{n} \lambda_i \alpha_i \exp[-\lambda_i t] \qquad (4)$$

For the given daughter isotope, the N1S method obtains probabilities using Equation 4 at each of the decay times in the problem.

As the photon energies (and therefore particle trajectory) are independent of decay time, instead of starting photons at each of the decay times in the problem, the N1S method only banks a single set of decay photons for a given decay chain. This increases the codes efficiency. The probability of the decay occurring at the decay time of interest is only taken into account when tallying. When the photons reach a tally a response is added to each of its decay time bins. The response for each time bin is weighted by the probability of the decay occurring at that decay time.

The N1S method has currently been implemented into MCNP6 [17], however the main N1S library, which reads the decay nuclear data and samples gammas, is code agnostic and can at a later date be incorporated into other transport codes which support time dependence and coupled neutron photon transport.

3. Verification

3.1. FNG ITER Shutdown Dose Rate Benchmark

3.1.1. Description

One of the most useful fusion relevant shutdown dose rate benchmarks was carried out at the Frascati Neutron Generator (FNG) in the year 2000. The full details of the experiment were written up in the Shielding Integral Benchmark Archive and Database (SINBAD) [18] and are summarised here. The FNG ITER SDDR benchmark has been used previously to validate various SDDR codes including MCR2S [7], D1SUNED [2] and R2SMESH [8] for fusion applications.

The FNG accelerates a deuteron beam up to 300 keV and focuses them onto a tritiated target to produce 14.1 MeV neutrons. The two experimental campaigns carried out during the year 2000 irradiated a material assembly designed to create a neutron flux spectrum similar to that anticipated in the outer vacuum vessel region of ITER. After irradiation the shutdown dose rate was measured at various decay times in the central cavity.

A layout of this assembly can be seen in Figure 2. The block consisted of layers of stainless steel and water-equivalent (perspex) material. The nominal size of the block was 714 mm x 1000 mm x 1000 mm.
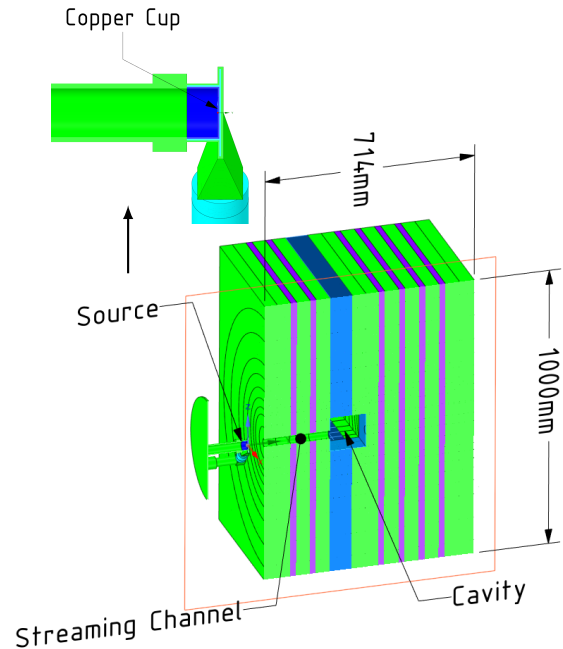
Figure 2: Layout of the fng mcnp model. Green and Blue: Steel, Purple: Perspex

N1S calculations were performed for both campaigns to calculate the shutdown dose rate in the detectors inserted into the cavity. The N1S calculations used the FENDL3.1d [19] nuclear

data cross-section library for transport calculations. For the decay library the N1S code used decay 2020 [12]. For metastable branching ratios the N1S calculations used TENDL2019 data.

3.1.2. Campaign 1

For Campaign 1 the block of steel and perspex was irradiated for a total of 18 hours over 3 days, resulting in a production of 1.815×10^{15} neutrons. The irradiation schedule used in the N1S calculation is given in Table 1.

Strength (n/s)	Duration (s)
2.32×10^{10}	19 440
0.00	61 680
2.87×10^{10}	32 940
0.00	54 840
1.90×10^{10}	15 720
0.00	6360
1.36×10^{10}	8940

Table 1: FNG irradiation scenarios for Campaigns 1

At the end of the irradiation an access port plug was removed from the side of the assembly and a Geiger-Muller detector inserted along with thermoluminescent dosimeter to measure the dose rates inside the cavity. Due to the current limitation in the N1S method, it is not possible to change the geometry that the irradiating neutrons and subsequent decay gammas see. Therefore the model used in the N1S calculation was that seen by the irradiating neutrons. This means that the access port plug was in place for the entire calculation and the aluminium shell of the Geiger-Muller detector was not present. These are unlikely to have a significant impact on the results as the activation of the plug does not dominate the dose rate in the chamber and the shielding effect on the total number of photons of 1 mm of aluminium will be negligible. Future modifications to the N1S method will allow for some differences between the irradiated geometry and the geometry the decay gammas see, allowing detector responses to be modelled directly in the N1S calculation.

The experimental results recorded by the Geiger-Muller tube [20] at various decay times are given in Table 2. Along with the experimental results the N1S calculated results are also given in Table 2. These have been estimated using the ANSI/ANS1991 [21] dose conversion factors which have been used previously [7] in analysis of the FNG benchmark.

Decay Time	Experiment		N1S	
Days	Dose (μSv/h)	Error	Dose (μSv/h)	Error
1	2.46E+00	2.46E-01	3.31E-06	2.84E-08
7	6.99E-01	6.99E-02	6.39E-07	1.98E-09
15	4.95E-01	4.95E-02	4.98E-07	1.10E-09
30	4.16E-01	4.16E-02	4.26E-07	9.37E-10
60	3.16E-01	3.16E-02	3.29E-07	6.91E-10

Table 2: Shutdown dose rate in the cavity of the FNG mock-up (results in μSv/h and errors are the statistical error on the N1S calculation)
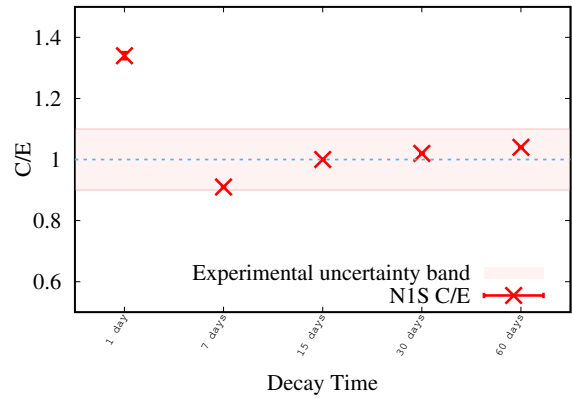
Figure 3: Campaign 1 Shutdown dose rate C/E values at various decay time

The calculated and experimental values are compared in a C/E (calculated/experimental) plot in Figure 3. It can be seen that the N1S method gives good agreement, within the experimental error, to the experimental results all but the 1 day decay time. This gives confidence that the N1S routines are working correctly. In order to ascertain the reason for the over prediction by the N1S method, analysis was carried out to determine the nuclides which dominate the response at each of the decay times. Additional code was written to allow the contribution from each daughter nuclide to be ascertained. A plot of the dominant nuclides driving the dose rate in the cavity at each decay time is given in Figure 5.
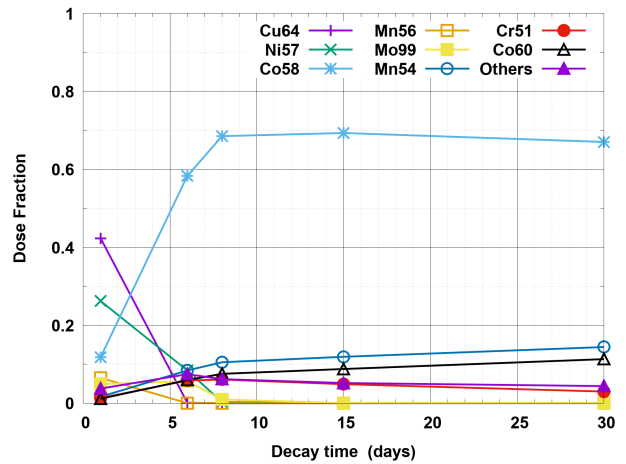
Figure 4: Campaign 1 dominant daughter nuclides contribution to the total dose rate at each decay time

Figure 5 shows that for the 1 day decay time the dose rate is dominated by ^{64}Cu which contributes about 42% of the dose. Although there is a small copper impurity in the steel slabs FISPACT-II calculations show that this only makes up 1.7% of the contact dose rate in the steel and will therefore not have a significant impact on the dose rate recorded in the cavity. The main source of ^{64}Cu comes from the ^{65}Cu(n,2n)^{64}Cu reaction within the copper cup of neutron generator, with photons then streaming down the streaming channel and into the cavity. Due

to its position this reaction is likely to be highly sensitive to the neutron source term used in the calculations which was a derived MCNP 'SDEF' source. Further work to improve the accuracy of the calculations should look at modifying the external FNG source routine to have time dependence (to allow it to be used with the N1S method) and improving the physics models used to calculate the neutron energise and angular dependence.

At decay times >1 day the dose rate is dominated by [58]Co with smaller contributions from [54]Mn and [60]Co.

3.1.3. Campaign 2

For Campaign 2 the steel and perspex block was irradiated for a total of 13 hours over two days, resulting in a total neutron production of 1.95×10^{15}. The irradiation schedule used in the N1S calculations was taken from the SINBAD database and is given in Table 3.

Strength (n/s)	Duration (s)
3.04×10^{10}	17 480
4.28×10^{10}	7820
0.00	54 140
4.29×10^{10}	22 140
0.00	900
3.78×10^{10}	3820
0.00	420
2.86×10^{10}	140

Table 3: FNG irradiation scenarios for Campaign 2

After the irradiation the access port plug was removed from the side of the assembly and a special plastic scintillator (NE 105) [20] inserted in order to estimate the shutdown dose. Also inserted was a NE 213 liquid scintillator to measure the gamma spectrum. Along with the removal of the access port plug a shield block was also placed across the opening of the streaming channel through the block to stop photons from the activated neutron generator significantly effecting the results (as was seen in Campaign 1 at the 1 day cooling time). Although a description of this shield block is not given in the text of the original benchmark documentation [20] it can be seen in Figure 7d [20], repeated here in Figure **??**, showing the MCNP model of the gamma transport calculations in the second irradiation campaign.

Like Campaign 1, the geometry used for the N1S method was that seen by the irradiating neutrons with the access port plug installed, without the shield across the streaming channel and without the detectors present in the cavity. As previously mentioned it is unlikely that the presence of the access port plug and the absence of the detectors will have a significant impact on the results. However, the absence of the shield across the streaming channel will have a significant effect on results for decay times when ^{64}Cu from the activation of the copper cup on the neutron generator makes a significant contribution. It was therefore decided to do two N1S calculations to see the effect of the gammas from the copper cup. The first calculations had
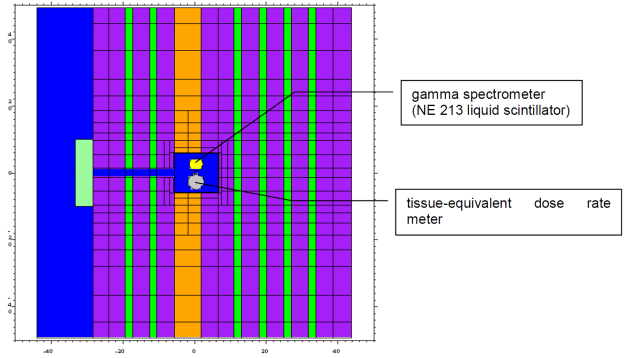
Figure 5: Campaign 2 shutdown layout taken from the benchmark documentation [20] showing the streaming channel shielding block in green.

the copper cup in the model and the second had the copper cup 'voided'.

The measured and calculated dose rates at times between 73 minutes and 20 days after irradiation are given in Table 4 and C/E values are plotted in Figure 6.

Decay Time	Experiment	MCNP With Cu		MCNP without Cu	
Secs	Dose (μSv/h)	Dose (μSv/h)	Error	Dose (μSv/h)	Error
4380	4.88E+02	4.03E+02	5.64E-01	3.92E+02	6.67E-01
6180	4.15E+02	3.53E+02	4.94E-01	3.43E+02	5.84E-01
7488	3.75E+02	3.20E+02	4.49E-01	3.12E+02	5.30E-01
11580	2.68E+02	2.38E+02	3.33E-01	2.31E+02	3.92E-01
17280	1.73E+02	1.57E+02	2.20E-01	1.52E+02	2.59E-01
24480	1.01E+02	9.41E+01	1.32E-01	9.04E+01	1.54E-01
34080	5.06E+01	4.86E+01	7.77E-02	4.60E+01	8.75E-02
45780	2.30E+01	2.30E+01	4.84E-02	2.13E+01	5.10E-02
57240	1.17E+01	1.23E+01	3.94E-02	1.10E+01	4.05E-02
72550	5.80E+00	6.66E+00	3.33E-02	5.64E+00	3.50E-02
90720	3.56E+00	4.40E+00	2.86E-02	3.65E+00	3.14E-02
132000	2.43E+00	3.04E+00	2.16E-02	2.64E+00	2.53E-02
212400	1.78E+00	2.15E+00	1.35E-02	2.02E+00	1.68E-02
345600	1.22E+00	1.49E+00	6.99E-03	1.46E+00	8.76E-03
479300	9.52E-01	1.18E+00	3.88E-03	1.16E+00	4.89E-03
708500	7.59E-01	9.40E-01	1.97E-03	9.29E-01	2.51E-03
1050000	6.67E-01	8.12E-01	1.38E-03	8.00E-01	1.76E-03
1670000	6.13E-01	7.26E-01	1.23E-03	7.15E-01	1.50E-03
1710000	6.14E-01	7.22E-01	1.23E-03	7.11E-01	1.49E-03

Table 4: Shutdown dose rate in the cavity of the FNG mock-up (results in μSv/h and errors are the statistical errors on the N1S calculation)

The C/E values show an underestimation up to about 20% at short decay times with up to a 20% overestimation at longer decay times. The decay times around 1 day (57,240 s to 212,400 s) are effected significantly by the copper cup in the neutron generator with smaller effects at shorter and longer decay times. The small deviations in the with and without the copper cup at shorter and longer decay times can be explained by the change in neutron flux and spectrum due to the lack of copper in the model.

The C/E results without the copper cup follow the same pattern seen in the original analysis of this benchmark [20] with an underestimation at short decay times rising to an over estimation at longer decay times. To see which nuclides dominate at the various decay times, a calculation was performed (with the copper cap in place). The results of this calculation can be seen in Figure 7

The dominant nuclide at short decay times is [56]Mn created
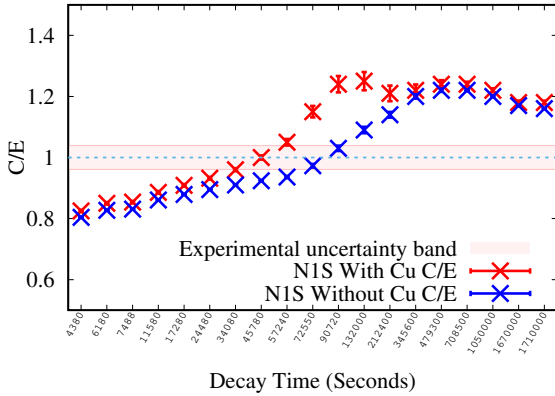
Figure 6: C/E plots of the shutdown dose rate for Campaign 2 at various decay times.
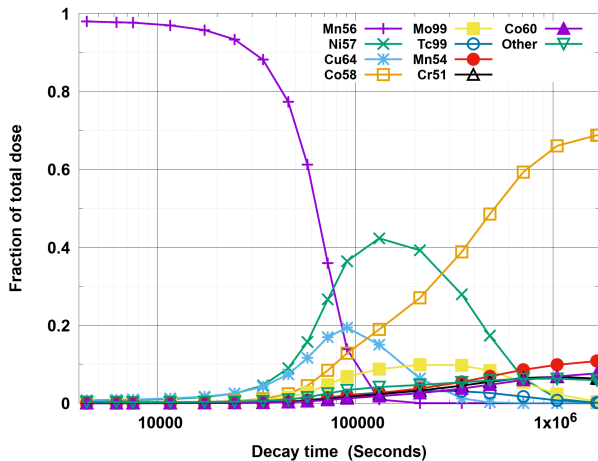
Figure 7: Campaign 1 dominant daughter nuclides contribution to the total dose rate at each decay time.

from the ^{56}Fe(n,p)^{56}Mn within the steel. At decay times between 90,720 s and 212,400 s the dose rate in the cavity is dominated by ^{57}Ni from the ^{58}Ni(n,2n)^{57}Ni reaction. At decay times longer than 345,600 s the dose rate is dominated by ^{58}Co which mainly comes from the ^{58}Ni(n,p)^{58}Co reaction. ^{64}Cu can be seen to make approximately 20% contribution to the dose rate at 132,000 s.

Along with the dose rate the gamma spectrum in the cavity was also measured using the NE 213 liquid scintillator. The spectrum was acquired and calculated with the N1S code at various decay times. The gamma spectrum at a decay time of 7,488 s and 708,500 s can be seen in Figure 8 and 9 respectively. It should be noted that the N1S results have been post processed to apply Gaussian broadening to the peaks as the detector is not present in the transport model and the spectra was recorded using an track length estimator (F4) tally. The Gaussian broadening applied was based on the Full-Width-Half-Maximum (FWHM) calculated from the peaks given in the experimental results.
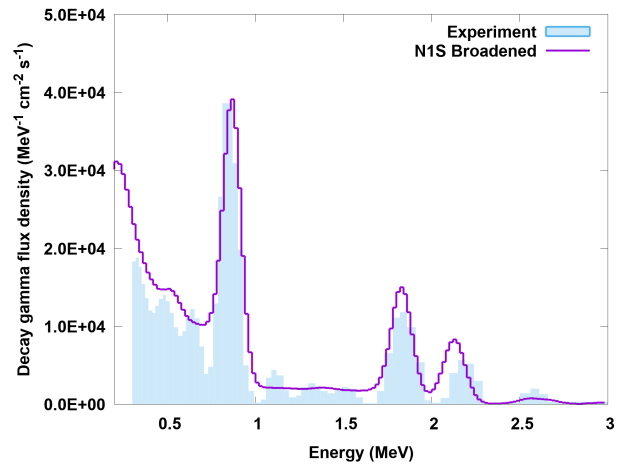
Figure 8: Gamma spectrum at a cooling time of 7,488 seconds (2.08 hours).

The three peaks associated with the ^{56}Mn decay can be clearly seen at 0.846 MeV, 1.81 MeV and 2.11 MeV in the gamma spectrum at 7448 s. The N1S broadened spectra matches the intensity of these peaks well although the experimental results at 2.11 MeV appears to be slightly shifted towards 2.2 MeV which is likely due to the energy calibration of the detector. This gives confidence that the code is correctly predicting the gammas from the ^{56}Mn decay.

The main peak seen in Figure 9 is the 0.810 MeV peak from ^{58}Co. A smaller 0.511 MeV annihilation peak can also been seen which is most likely from the electron capture decay of ^{58}Co. The N1S broadened spectra again matches the experimental data well with the peak intensities and locations agreeing. There is a discrepancy at lower energies principally due to two effects; the lack of detector model in the simulation and the use of an F4 tally which will not take account of x-rays created in the housing of the detector, nor the partial deposition of energy due to compton scattering by photons in the detector.

7
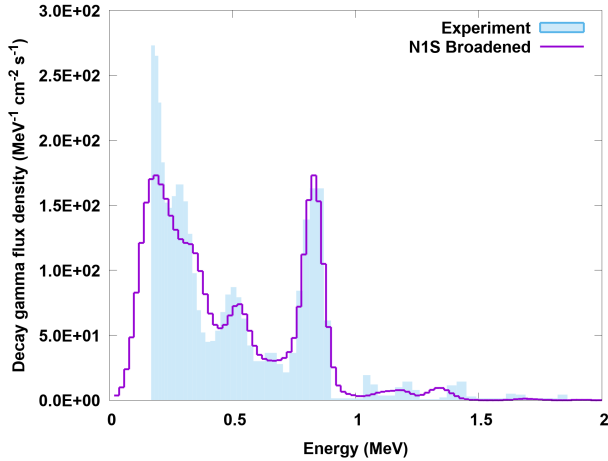
Figure 9: Gamma spectrum at a cooling time of 708,500 seconds (8.2 days).

3.2. ITER SDDR Cross Comparison

3.2.1. Description

The ITER SDDR Code Cross Comparison [22] is based on an ITER port plug like geometry and has been used previously [23][2][8] to demonstrate the applicability of SDDR codes to an ITER like geometry. Although the geometry is relatively simple, it does include some of the important features that need to be considered when calculating the SDDR in an ITER port interspace such as streaming gaps and heavily shielded regions. The geometry consists of three concentric cylinders which can be seen in Figure 10. An outer steel cylinder (of outer radius 100 cm and inner radius of 50 cm) surrounds a steel and water cylinder (of thickness 210 cm and, outer and inner radii of 48 and 7.5 cm respectively) at the front of the assembly and a steel plate (of 15 cm thickness and an outer radius of 48 cm) at the rear of the assembly.
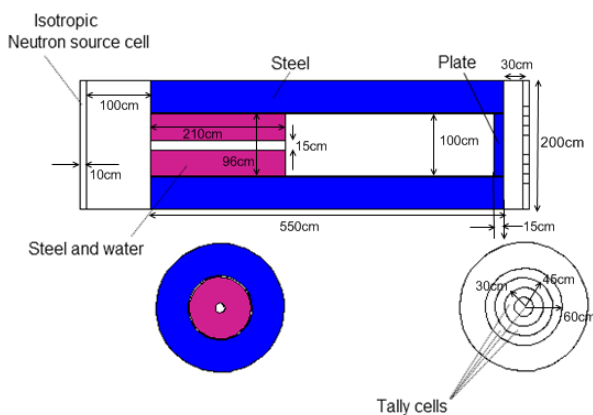
Figure 10: Layout of the ITER computational benchmark.

The neutron source is a 14 MeV isotropic volume source of 100 cm radius and 10 cm thickness positioned 100 cm away from the front face of the assembly. The neutron source has a nominal intensity of $2x10^{19}$ n/s and irradiates the cylinders following the schedule given in Table 5.

Source Strength (n/s)	Duration	Repetitions
1.07×10^{17}	2 years	1
8.25×10^{17}	10 years	1
0	0.667 years	1
1.66×10^{18}	2 years	1
0	3920 sec	17
2.00×10^{19}	400 sec	
0	3920 sec	4
2.80×10^{19}	400 sec	

Table 5: ITER computational benchmark irradiation scenario.

After irradiation the SDDR is recorded at a decay time of 10^6 s in five tally cells 30 cm away from the far end of the assembly. These tally cells are concentric annular tallies with a thickness of 10 cm and an outer radii of 15, 30, 45, 60 and 100 cm respectively. Track length estimator (F4) tallies were used for each of the cell volumes and modified by the ICRP 74 photon flux to effective dose conversion factors [24] (calculated for the Antero-posterior geometry by calculating the product of the effective dose per unit kerma free-in-air and the air kerma per unit fluence).

Previous analysis of this benchmark by UKAEA [23], UNED [2] and KIT[8] have shown that MCR2S, R2SMesh, R2SUNED and D1SUNED all give similar answers. These all used FENDL 2.1 [25] or 3 [26] cross sections for the neutron transport, EAF 2007 [27] or 2010 [14] cross sections for the neutron activation and MCLIB84 [28] nuclear data for the photon transport.

The calculations documented here with the N1S method used the FENDL3.2 neutron and the MCLIB84 photon cross section libraries. The metastable state branching ratios used were produced from the EAF2010 activation library in 175 Vitamin-J energy groups.

3.2.2. Results

The SDDR calculated by the N1S method in the concentric cylinders at the end of the assembly are given in Table 6 and Figure 11 . Along with the SDDR calculated by the N1S method, two sets of SDDR values calculated using the MCR2S cell under voxel method are also provided for comparison. The first set of MCR2S results were calculated using EAF2010 activation data in 175 Vitamin-J energy groups, which matched previous assessments of this cross comparison [23]. The second set of MCR2S results were calculated using TENDL2019 [29] activation data in 709 energy groups.

The N1S method predicts dose rates which are up to 8% below the values predicted by MCR2S using EAF2010 activation data. However, the N1S method gives excellent agreement, within 1% for all tallies apart from 45<r<60 cm which has a 4% difference, with MCR2S using TENDL2019 activation data.

In order to understand why this difference occurs subsequent analysis was performed. The majority of the contributions to the dose tallies at the end of the assembly comes from the acti-

8

Radius	MCR2S EAF		MCR2S TENDL		N1S	
	Dose (Sv/h)	Error	Dose (Sv/h)	Error	Dose (Sv/h)	Error
<15 cm	1.63E-02	6.52E-05	1.52E-02	1.42E-04	1.50E-02	5.49E-04
15<r<30 cm	1.32E-02	3.30E-05	1.22E-02	6.86E-05	1.23E-02	4.01E-04
30<r<45 cm	9.01E-03	2.07E-05	8.39E-03	4.03E-05	8.28E-03	2.56E-04
45<r<60 cm	5.68E-03	1.31E-05	5.37E-03	2.90E-05	5.56E-03	3.42E-04
r>60 cm	2.25E-03	4.50E-06	2.11E-03	8.42E-06	2.08E-03	6.56E-05

Table 6: ITER computational benchmark SDDR cell tally results comparison (results in Sv/h). Note that errors associated with the MCR2S dose rate results only include the statistical error on the photon transport calculation. The errors in the N1S results are the statistical error on the photon results from the combined neutron-photon calculation
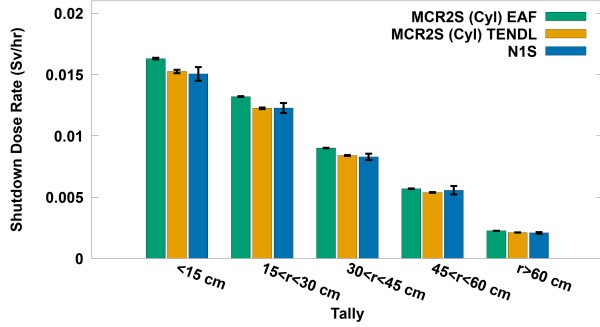
Figure 11: ITER computational benchmark SDDR cell tally results comparison, error bars represent the statistical uncertainty on the gamma transport calculation for MCR2S calculations and the statistical error on the dose tallies in the N1S calculation.

vation of the 15 cm thick steel plate and the activation of the rear of the outer steel cylinder at the end of the assembly. Therefore the neutron flux and spectra (in 175 and 709) were recorded in the steel plate. These were used to perform FISPACT-II calculations to determine the contact dose rate in the rear steel plate and ascertain which isotopes and reactions dominate the dose rate. The contact dose rate (estimated using a semi-infinate slab model [5]) and the dominant isotopes seen in Table 7 for EAF2010 and TENDL2019.

	Dose Contribution %	
Daughter Isotope	EAF2010	TENDL2019
^{58}Co	54.18	55.11
^{54}Mn	29.49	28.10
^{60}Co	11.52	11.71
^{57}Co	1.80	2.07
^{182}Ta	0.97	0.94
Contact Dose (Sv/h)	6.41E-02	5.99E-02

Table 7: Dominant nuclides to the contact dose rate of the steel plate

From Table 7 it can be seen that the contact dose rate predicted by EAF2010 is approximately 7% higher than TENDL2019. This is approximately the same difference seen in the SDDR tallies at the rear of the assembly. Over 90% of this dose rate comes from the decay of three daughter isotopes, ^{58}Co, ^{54}Mn and ^{60}Co. The main reaction pathways that lead to these daughter isotopes are given in Table 8 along with the percentage contribution for each pathway to the daughter product

(calculated using the TENDL2019 library, although EAF values were similar) and the reactions rates calculated by each of the libraries.

Reaction	Contr. %	Reaction Rate (cm^{-3}s^{-1})		
		EAF2010	TENDL2019	FENDL3.2
^{58}Ni(n,p)^{58}Co	99	1.20E+07	1.14E+07	1.14E+07
^{55}Mn(n,2n)^{54}Mn	40	4.72E+06	4.16E+06	4.07E+06
^{54}Fe(n,p)^{54}Mn	59	6.76E+06	6.08E+06	6.07E+06
^{59}Co(n,γ)^{60}Co	22	5.35E+05	4.76E+05	4.52E+05
^{60}Ni(n,p)^{60}Co	76	1.71E+06	1.65E+06	1.59E+06

Table 8: Reaction Rates for dominant nuclides estimated by TENDL2019, FENDL3.2 and EAF2010 in the steel plate at the end of the assembly (Note that the % pathway contribution to the reaction product is derived from the TENDL Library)

The ratios between the reactions rates calculated by the different libraries can be seen in Figure 12. From this it can be seen that the TENDL2019 reaction rates closely match those given by FENDL3.2.
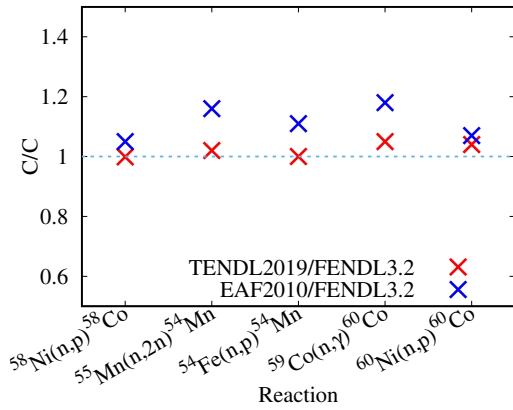
Figure 12: Reaction rate ratios for TENDL2019/FENDL3.2 and EAF2010/FENDL3.2 in the steel plate at the end of the assembly

For the first 3 reaction pathways listed in Table 8, which lead to >80% of the the dose, the reaction rates calculated using TENDL2019 and FENDL3.2 are in very good agreement with a maximum difference of 2% for the ^{55}Mn(n,2n)^{54}Mn reaction. The difference between TENDL2019 and FENDL3.2 in the two reaction pathways leading to Co60 is up to 5%. To estimate the combined effect these reaction rate differences have on the dose rate (ΔDR), Equation 5 was used.

$$\Delta DR = \sum_{i=1}^{n} \Delta RR_i C_i^d C_d^{dose} \qquad (5)$$

Where n is the number of reaction pathways, ΔRR_i is the difference between the reaction rates (calculated using Equation 6) for pathway i, C_i^d is the fractional contribution to the daughter (d) of reaction pathway i and C_d^{dose} is the fractional contribution made to the dose rate of daughter d.

$$\Delta RR = \frac{RR_1 - RR_2}{RR_1} \qquad (6)$$

Where RR_1 is the reaction rate calculated by the first library and RR_2 is the reaction rate calculated by the second library.

Using Equation 5 with TENDL2019 as the first library and FENDL3.2 as the second library the difference in dose rate caused by the differences in the reaction rates is <1%. This agrees with the SDDR values in Table 6 which are generally within 1% of each other for the N1S and MCR2S calculation using TENDL2019.

The reaction rate differences between EAF2010 and FENDL3.2 are larger, with the difference for ^{58}Ni(n,p)^{58}Co being 5%, ^{55}Mn(n,2n)^{54}Mn being 14% and ^{54}Fe(n,p)^{54}Mn being 10%. For ^{60}Co production the reaction rate differences are 16% for ^{59}Co(n,γ)^{60}Co and 7% for ^{60}Ni(n,p)^{60}Co. Combining these reaction rate difference using Equation 5 gives a difference caused by the reaction rates in the dose of approximately 8%. This shows that most of the differences seen between the N1S method and MCR2S using EAF2010 and TENDL2019 data in Table 6 can be explained by differences in the calculated reaction rates.

The differences in reaction rates between EAF2010 and FENDL3.2 are caused by two reasons. The first is the EAF data when used with FISPACT-II requires the neutron spectrum to be descritised into 175 Vitamin-J energy group structure. This leads to some over prediction, especially in (n,γ) reactions where resonance and 1/v regions, and self shielding effects are important. The FENDL3.2 reaction rates calculated with MCNP use continuous point-wise cross-section data and can account for self-shielding effects. The second reason for the differences in reaction rates are differences in the cross section data used. An example of these difference can be see in Figure 13 which shows the a plot of the point-wise cross section data for the ^{55}Mn(n,2n)^{54}Mn reaction from each of the three nuclear data libraries. These show that for the region up to 17 MeV the EAF2010 cross section is higher than both the FENDL3.2 and TENDL2019 cross sections. As the source in the ITER SDDR cross comparison is 14 MeV this leads to a higher ^{55}Mn(n,2n)^{54}Mn reaction rate, and subsequent SDDR, when the EAF2010 data is used.
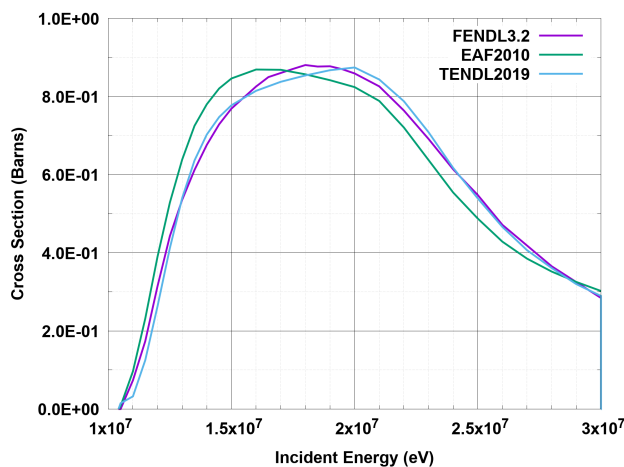
Figure 13: ^{55}Mn(n,2n)^{54}Mn Cross section

4. Discussion and Conclusions

A new shutdown dose rate methodology has been created and implemented into a computational library for use in radiation transport codes, here described as the N1S method. This methodology and subsequent library has been incorporated in to MCNP and validated against the FNG ITER Shutdown Dose Rate Benchmark and the ITER SDDR cross comparison model.

The N1S method allows the calculation of the shutdown dose rates and other shutdown responses in a single calculation. This allows the code to take full account of self-shielding effects calculated in the transport code as well as correct spatial handling of source photons.

The N1S method removes one of the main disadvantages of the D1S method, notably the need to pre-calculate time correction factors and have prior knowledge of the important nuclides that would contribute to dose rate estimates at cooling times of interest. This opens up the code to be deployed in automated workflows as no analyst input is required. It also eliminates the possibility of accidentally missing important isotopes which could lead to incorrect results.

The N1S method was used to calculate the SDDR in the central cavity of the FNG ITER SDDR Benchmark. Results for Campaign 1 were shown to be within the range of the experimental error for all, apart from the 1 day, decay times. The N1S result at the 1 day decay time has a C/E of approximately 1.3. This was shown to be due to ^{65}Cu(n,2n)^{64}Cu reaction in the copper cup of the neutron generator.

The N1S results for Campaign 2 were shown to be underestimated, by up to 20%, at short decay times where ^{56}Mn dominates the dose field and overestimated, by up to 20%, at longer decay times where ^{58}Co dominates, when compared to the experimental results. The effects of excluding the copper cup in the Campaign 2 MCNP model (to account for the addition of a shield across the streaming path during shutdown) was shown to significantly improve agreement between the N1S calculated values and the experiment for decay times between 57,240 s to 212,400 s.

The N1S code showed good agreement with other shutdown dose rate codes for the ITER cross comparison. The N1S code was shown to have differences up to 8% when compared to MCR2S using EAF2010 nuclear data library and mainly <1% when compared to the MCR2S using the TENDL2019 nuclear data library. The larger difference seen when comparing to MCR2S using EAF2010 were shown to be due to deviations in the reaction rates predicted through use of the FENDL3.2 and the EAF2010 nuclear data libraries.

One current limitation of the N1S method is lack of flexibility in being able to change the model between the on-load configuration, seen by the neutrons, and shutdown configuration, seen by the decay photons. In future developments it planned to allow for changes in the material composition of components between the on-load neutrons and decay photons. This will allow for modifications to be made to the geometry during shutdown. In the case of the FNG SDDR experiment this will allow for more accurate modelling as the access plug to be could be removed, the detector installed and the shield across

the streaming path added. This function would also be useful for the assessment of fusion reactors during maintenance where components are regularly removed and drained of coolant.

The N1S methodology has been demonstrated to show good agreement and capability for SDDR calculations and with further development, the N1S method has the possibility to become an excellent diagnostics tool allowing the analyst to ascertain the dominant isotopes and locations leading to the shutdown response of interest. A dominant isotope identification procedure has already been implemented as can be seen in Sections 3, with further developments required to improve the user interface. As the location of the reactions leading to the dominating photons is known in the code it would relatively straight forward to record this data and output it allowing for regions of the geometry important to the shutdown response of interest to be identified. The way the N1S library has been written it will also be relatively straight forward to implemented into other time dependent radiation transport codes such as OpenMC version 0.13.0 or greater.

Acknowledgements

References

[1] R. Villari, P. Batistoni, S. Conroy, A. Manning, F. Moro, L. Petrizzi, et al., Shutdown dose rate benchmark experiment at JET to validate the three-dimensional Advanced-D1S method, Fusion Engineering and Design 87 (2012) 1095–1100.

[2] P. Sauvan, R. Juárez, G. Pedroche, J. Alguacil, J. P. Catalan, F. Ogando, J. Sanz, D1suned system for the determination of decay photon related quantities, Fusion Engineering and Design 151 (2020) 111399.

[3] X-5 Monte Carlo Team, MCNP - A General Monte Carlo N-Particle Transport Code, Version 5, LA-CP-03-0245.

[4] C. J, Werner, MCNP User's Manual, Code Version 6.2, LA-CP-17-29981.

[5] J.-C. Sublet, J. Eastwood, J. Morgan, The FISPACT-II user manual, CCFE-R (11) 11.

[6] Y. Chen, U. Fischer, Rigorous MCNP based shutdown dose rate calculations: computational scheme, verification calculations and application to ITER, Fusion Engineering and Design 63/64 (2002) 107–114.

[7] A. Davis, R. Pampin, Benchmarking the MCR2S system for high-resolution activations dose analysis in ITER, Fusion Engineering and Design 85 (2010) 87–92.

[8] M. Majerle, D. Leichtle, U. Fischer, A. Serikov, Verification and validation of the R2Smesh approach for the calculation of high resolution shutdown dose rate distributions, Fusion Engineering and Design 87 (2012) 443–447.

[9] P. Sauvan, J. Catalan, F. Ogando, J. S. Recio, Development of the R2SUNED code system for shutdown dose rate calculations, IEEE Transactions on Nuclear Science 63 (2016) 375–384.

[10] M. Herman, A. Trkov, ENDF-6 formats manual, Brookhaven National Laboratory Report BNL-90365-2009 Rev.1.

[11] decay_2012 available at https://fispact.ukaea.uk/nuclear-data/downloads/, UKAEA.

[12] decay_2020 available at https://fispact.ukaea.uk/nuclear-data/downloads/, UKAEA.

[13] J. L. Conlin, F. B. Brown, A. C. Kahler, M. B. Lee, D. K. Parsons, M. C. White, Updating the format of ACE data tables, LANL LA-UR-12-22033.

[14] J.-C. Sublet, L. Packer, J. Kopecky, R. A. Forest, A. Koning, D. Rochman, EAF 2010 neutron-induced cross section library, CCFE-R (10) 05.

[15] J. Cetnar, General solution of bateman equations for nuclear transmutations, Annals of Nuclear Energy 33 (2006) 640–645.

[16] H. Bateman, Solution of a system of differential equation occurring in the theory of radioactive transformations, Proc. Cambridge Philos. Soc. 15 (1910) 423–427.

[17] D. B. Pelowitz, MCNP user's manual code version 6.2, LA-UR-17-29981.

[18] I. Kodeli, E. Sartori, B. Kirk, SINBAD shielding benchmark experiments status and planned activities, ANS 14th Biennial Topical Meeting of the Radiation Shielding Protection and Shielding Division.

[19] R. A. Forrest, C. K. Walker, M. Avirigeanu, A. V. Ignatyuk, F. Tarkanyi, A. Trkov, J. Kopecky, U. Fischer, FENDL-3 library, INDC(NDS)-0645.

[20] P. Batistoni, M. Angelone, L. Petrizzi, M. Pillon, H. Freiesleben, D. Richter, K. Seidel, S. Unholzer, Y. Chen, U. Fischer, Experimental validation of shut-dose dose rates final report, ITER Task T-426.

[21] American National Standard, Neutron and gamma-ray fluence-to-dose factors, ANSI/ANS-6.1.1-1991.

[22] M. Loughlin, Conclusions of shutdown dose rate benchmark study, IDM Number: 6593RF v1.0, 6th ITER Neutronics Meeting, Hefei, China.

[23] T. Eade, B. Colling, J. Naish, L. W. Packer, A. Valentine, Shutdown dose rate benchmarking using modern particle transport codes, Nuclear Fusion 60 (2020) 5.

[24] ICRP, Conversion coefficients for use in radiological protection against external radiation, Annals of the ICRP Publication 74.

[25] D. L. Aldama, A. Trkov, Fendl-2.1, update of an evaluated nuclear data library for fusion applications, INDC(NDS)-467.

[26] R. Forrest, R. Capote, N. Otsuka, T. Kawano, A. Koning, S. Kunieda, J.-C. Sublet, Y. Watanabe, FENDL-3 library summary documentation, INDC(NDS)-0628.

[27] R. A. Forrest, J. Kopecky, J. Sublet, The european activation file: EAF-2007 neutron-induced cross section library, UKAEA FUS 535.

[28] M. C. White, Further notes on MCPLIB03/04 and new MCPLIB63/84 compton broadening data for all versions of mcnp5, LANL LA-UR-12-00018.

[29] A. J. Koning, D. Rochman, J. Sublet, N. Dzysiuk, M. Fleming, S. van der Marck, TENDL: Complete nuclear data library for innovative nuclear science and technology, Nuclear Data Sheets 155 (2019) 1.